

Isotope Effects in Dissociative Excitation of C₂H₂ and C₂D₂ by Collisions with Metastable Ne(³P_{0,2}) Atoms

Masaharu TSUJI^{*1,2†} Takahiro KOMATSU^{*3} Keiko UTO^{*1}

Jun-Ichiro HAYASHI^{*1,2} and Takeshi TSUJI^{*4}

^{*†}E-mail of corresponding author: tsuji@cm.kyushu-u.ac.jp

(Received May 24, 2021, accepted June 7, 2021)

Isotope effects in dissociative excitation of C₂H₂ and C₂D₂ by collisions with metastable Ne(³P_{0,2}) atoms have been studied in the Ne flowing afterglow. The CD(A²Δ-X²Π_r, B²Σ⁻-X²Π_r, and C²Σ⁺-X²Π_r) and C₂(d³Π_g-a³Π_u, C¹Π_g-A¹Π_u, e³Π_g-a³Π_u, and D¹Σ_u⁺-X¹Σ_g⁺) emission systems have been identified in the UV and visible region. The emission rate constants of CD(A,B,C) and C₂(d,C,e,D) were determined to be 1.7, 0.25, 0.014, and 5.4, 0.39, 0.12, 0.0046 × 10⁻¹³ cm³ molecule⁻¹ s⁻¹, respectively. The isotopic ratios of k_H(CH^{*})/k_D(CD^{*}) and k_H(C₂^{*})/k_D(C₂^{*}) were determined to be 0.85 and 1.73, respectively. Although the reduction of emission rate constant of C₂^{*} from C₂D₂ is consistent with a simple dissociation model from the RRKM theory, the increase in the emission rate constant of CD^{*} does not agree with it. The *inverse* isotope effect for CD^{*} is explained by the fact that the formation of C₂^{*} and CH^{*} or CD^{*} occurs competitively, so that faster dissociation of C-H bonds suppresses the formation of CH^{*}. Other possible mechanisms to explain the *inverse* isotope effect for CD^{*} are discussed. The nascent vibrational and rotational distributions of CD(A:v'=0-2,B:v'=0) and C₂(d:v'=0-6, C:v'=0-3, e:v'=0-6, D:v'=0-2) were determined and compared with those obtained in the Ne(³P_{0,2})/C₂H₂ reaction.

Key words: Isotope effect, Dissociative excitation, Acetylene, Metastable Ne* atoms, Emission rate constant, Rovibrational distribution, Superexcited state, Reaction dynamics

1. Introduction

In a preceding paper, we have studied the energy-transfer reaction of Ne(³P_{0,2}) with C₂H₂ in the Ne flowing afterglow.¹⁾ The CH(A²Δ-X²Π_r, B²Σ⁻-X²Π_r, and C²Σ⁺-X²Π_r) and C₂(d³Π_g-a³Π_u, C¹Π_g-A¹Π_u, e³Π_g-a³Π_u, and D¹Σ_u⁺-X¹Σ_g⁺) emission systems have been observed in the UV and visible region. Emission rate constants of CH(A,B,C) and C₂(d,C,e,D) were determined by using a reference reaction method. Rovibrational distributions of CH(A,B) and C₂(d,C,e,D) were determined from computer simulation of observed spectra. Significant vibrational excitation of C₂^{*} and rotational excitation of CH^{*} and C₂^{*} were observed. When the observed vibrational and rotational distributions of CH(A,B) and C₂(d,C,e,D) were

compared with statistical prior ones, large discrepancies were observed in most cases. These results suggested that CH^{*} and C₂^{*} fragments are not formed through long-lived near-resonant C₂H₂^{**} states, where excess energies are distributed in all internal degrees of freedom statistically. It was concluded that the most important factor, which dominates the reaction dynamics, is molecular structure of precursor state. CH(A,B) and C₂(d,C,e,D) are formed via *trans*-bent near-resonant Rydberg states converging to the first excited \tilde{A} ²A_g state of C₂H₂⁺. Non-linear precursor superexcited states with enlarged C≡C bond and excited CCH bending vibration led to vibrationally excited C₂^{*} and rotationally excited CH^{*} and C₂^{*} fragments.

In the present study, UV and visible emission spectra resulting from the Ne(³P₂: 16.62 eV, 3P₀: 16.72 eV)/C₂D₂ reaction are measured in the Ne afterglow to obtain more information on the reaction dynamics from isotope effects. The emission rate constants of each emitting state and rovibrational distributions of excited states are determined and compared with those obtained from the Ne(³P_{0,2})/C₂H₂ reaction.¹⁾

*1 Institute for Materials Chemistry and Engineering, and Research and Education Center of Green Technology

*2 Department of Applied Science for Electronics and Materials

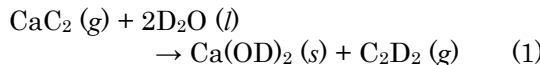
*3 Department of Applied Science for Electronics and Materials, Graduate Student

*4 Department of Materials Science, Shimane University

Isotope effects obtained are also compared with those reported in vacuum ultraviolet (VUV) photoexcitation with similar excitation energies.^{2,3)}

2. Experimental

The FA apparatus equipped with UV and visible optical emission detection system was the same as that reported in the preceding paper.¹⁾ C₂D₂ was synthesized by the reaction of CaC₂ with D₂O using a liquid nitrogen to suppress a rapid reaction.



Purity of CaC₂ and D₂O reagents were higher than 99.9%. The partial pressure of C₂D₂ in the reaction zone was 1–6 mTorr (1 Torr = 133.3 Pa).

3. Results

3.1 Emission spectra and dissociative excitation processes

Figure 1a shows a typical emission spectrum obtained from the Ne afterglow reaction of C₂D₂. The CD(A²Δ–X²Π_r) and B²Σ[–]–X²Π_r) and C₂(d³Π_g–a³Π_u) and C¹Π_g–A¹Π_u) emission systems are identified in the 330–570 nm region. In addition, CD(C²Σ⁺–X²Π_r) and C₂(e³Π_g–a³Π_u) and D¹Σ_u⁺–X¹Σ_g⁺) emission systems are identified in the 314 nm and 210–300 nm region, respectively (not shown in Fig. 1a). For comparison, emission spectrum obtained from the Ne(³P_{0,2})/C₂H₂ reaction is shown in Fig. 1b, where corresponding CH(A–X) and B–X) and C₂(d–a) and C–A) emission systems are observed. The most outstanding

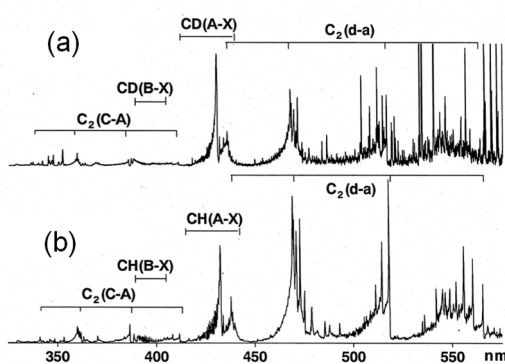
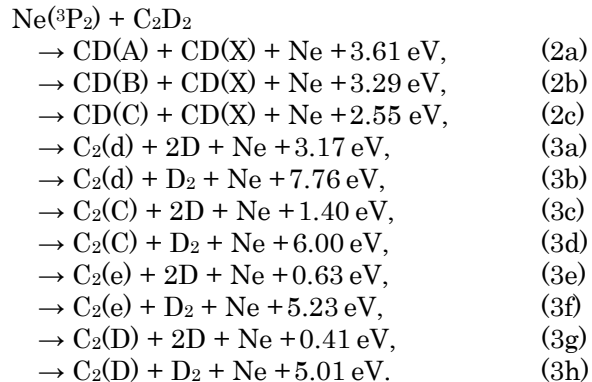


Fig. 1. Emission spectra obtained from the (a) Ne(³P_{0,2})/C₂D₂ and (b) Ne(³P_{0,2})/C₂H₂ reactions.

feature of the Ne(³P₂)/C₂D₂ spectrum is that the intensity ratio of C₂(d–a)/CD(A–X) becomes small in comparison with that of C₂(d–a)/CH(A–X) in the Ne(³P_{0,2})/C₂H₂ reaction.

3.2 Emission rate constants of CD* and C₂*

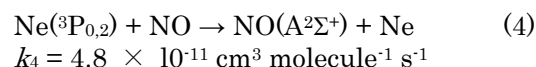
CD(A,B) and C₂(d,C,e,D) are formed from the following energy-transfer reactions between Ne(³P₂) atoms and C₂D₂:



The ΔH° values were calculated using reported thermochemical and spectroscopic data.^{4,5)} For the reactions with higher-energy Ne(³P₀) atoms, 0.10 eV higher excess energies are released in the above reactions. The excess energies released in the Ne(³P₂)/C₂D₂ reaction are smaller than those in the Ne(³P₂)/C₂H₂ reaction¹⁾ by 0.05–0.17 eV.

Among above processes, highly exoergic reactions (3b), (3d), (3f), and (3h), in which D₂ molecules are formed, will be unfavorable, because large excess energies should be released as rovibrational energies and kinetic energies of products.

The emission rate constants for reactions (2)–(3) were determined by using the reference reaction method reported in our previous paper.¹⁾ The Ne(³P_{0,2})/NO reaction was used as a reference reaction.



Emission rate constants of each species were estimated by comparing the integrated emission intensity of each band system with that of NO(A–X) in prepared mixtures of C₂D₂/NO. Results obtained are given in Table 1 along with our results for the Ne(³P_{0,2})/C₂H₂ reaction.¹⁾ If there is no nonradiative decay and pumping from the observation region, the emission rate constants equal the formation ones. Hereafter, k_H(X) and k_D(X) represent

Table 1. Emission rate constants of the excited fragments produced in the Ne(³P_{0,2})/C₂D₂ and Ne(³P_{0,2})/C₂H₂ reactions. ($\times 10^{-13}$ cm³ molecule⁻¹ s⁻¹).

Ne(³ P _{0,2})/C ₂ D ₂	<i>k</i> _D This work	Ne(³ P _{0,2})/C ₂ H ₂	<i>k</i> _H Ref. 1	<i>k</i> _H / <i>k</i> _D
CD(A)	1.7	CH(A)	1.5	0.88
CD(B)	0.25	CH(B)	0.22	0.88
CD(C)	0.014	CH(C)	0.0046	0.33
sum	2.0	sum	1.7	0.85
C ₂ (d)	5.4	C ₂ (d)	9.3	1.72
C ₂ (C)	0.39	C ₂ (C)	0.69	1.77
C ₂ (e)	0.12	C ₂ (e)	0.22	1.83
C ₂ (D)	0.0046	C ₂ (D)	0.0069	1.50
sum	5.9	sum	10.2	1.73
total	7.9	total	11.9	1.51

emission rate constants of excited species X produced from C₂H₂ and C₂D₂, respectively. The *k*_D(C₂*^{*}) and *k*_H(C₂*^{*}) values are larger than the *k*_D(CD*) and *k*_H(CH*) values by factors of 3.0 and 6.0, respectively. Here, C₂*^{*}, CD*, and CH* stand for C₂(d,C,e,D), CD(A,B,C), and CH(A,B,C), respectively. Results obtained imply that C₂*^{*} are more favorable excited products than CD* or CH* in the Ne(³P_{0,2})/C₂D₂ and Ne(³P_{0,2})/C₂H₂ reactions. Among CD(A,B,C) or CH(A,B,C) and C₂(d,C,e,D) products, the CD(A) or CH(A) and C₂(d) states are major product states. Actually, the *k*_D(CD(A)) and *k*_H(CH(A)) values occupy 85% and 88% of *k*_D(CD*) and *k*_H(CH*), whereas the *k*_D(C₂(d)) and *k*_H(C₂(d)) values occupy 92% and 91% of *k*_D(C₂*^{*}) and *k*_H(C₂*^{*}), respectively.

When deuterium isotope effects are examined, the following ratios are obtained for the total emission rate constants of CH* or CD* and C₂*^{*}.

$$k_H(CH^*) / k_D(CD^*) = 0.85 \quad (5a)$$

$$k_H(C_2^*) / k_D(C_2^*) = 1.73 \quad (5b)$$

It should be noted that the formation of CD(A,B,C) by C≡C scission is enhanced by the deuterium substitution, whereas the formation of C₂(d,C,e,D) by two C–D bond scissions are suppressed by the deuterium substitution. When the dependence of isotope ratio on the product state is examined, the isotope ratio of the major CH(A,B) states is the same (0.88),

whereas that of the minor CH(C) state is very small (0.33). The isotope ratios for the major C₂(d,C,e) states are nearly the same (1.72–1.83), whereas that for the minor highest C₂(D) state (1.50) is smaller than the above major states. These results show that the dependence of isotope effects on the CH* and C₂* electronic states is small for the major CH(A,B) and C₂(d,C,e) states. Based on the above facts, we believe that similar reaction dynamics takes part in the formation of CH* or CD* and C₂* from dissociation of C₂H₂** and C₂D₂** superexcited states. Further detailed discussion about isotope effects will be given in the Discussion section.

3.3 Rovibrational distributions of CD(A,B) and C₂(d,C,e,D) in the Ne(³P_{0,2})/C₂D₂ reaction

Rovibrational distributions of CD(A,B) and C₂(d,C,e,D) in the Ne(³P_{0,2})/C₂D₂ reaction were determined by a computer simulation of emission spectra. The simulation procedure was the same as that used in the Ne(³P_{0,2})/C₂H₂ reaction.¹⁾

In Figs. 2–7 are shown the observed and best fit spectra of the CD(A–X, B–X) bands and C₂(d–a, C–A, e–a, and D–X) bands obtained assuming single Boltzmann rotational distributions for each *v'* level. Vibrational distributions and rotational temperatures thus obtained for CH(A,B) and C₂(d,C,e,D) are given in Tables 2 and 3, respectively. From the observed rovibrational distributions, we estimated the average vibrational and rotational energies of each CD* and C₂* state, denoted as $\langle E_v \rangle$ and $\langle E_r \rangle$, and the average yields of total available energy into these degrees of freedom, denoted as $\langle f_i \rangle$ and $\langle f_r \rangle$, respectively. Symbol $\langle f_i \rangle$ represents the average yield of total available energy into the relative translational energy. The $\langle E_v \rangle$, $\langle E_r \rangle$, $\langle f_i \rangle$, $\langle f_r \rangle$, and $\langle f_t \rangle$ values obtained for CD* and C₂* are summarized in Tables 4 and 5, respectively. For comparison, corresponding data of CH* and C₂* obtained in the Ne(³P_{0,2})/C₂H₂ reaction¹⁾ are given.

On the basis of observed rovibrational distributions of CD* and C₂*, the following tendencies are found.

(A) Formation of CD*

- The vibrational population and rotational temperatures of CD(A:*v'*=0–2) are nearly the same as those of CH(A:*v'*=0–2) from C₂H₂¹⁾ except for a lower rotational temperature of 800 K for CD(A:*v'*=2). The

- rotational temperatures of CD(B: $v'=0$) is higher than that of CH(B: $v'=0$) by 25%.¹⁾
- (2) The $\langle E_v \rangle$ and $\langle f_v \rangle$ values of CH(A) are larger than those of CD(A) by 25–30%. The $\langle E_r \rangle$ and $\langle f_r \rangle$ values of CH(A) are nearly

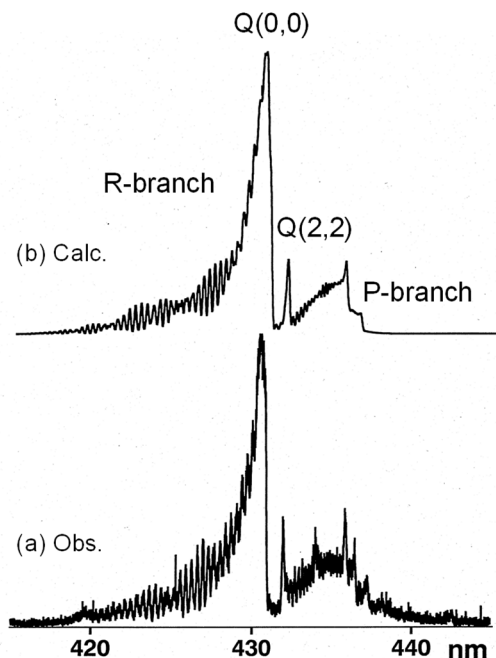


Fig. 2. (a) observed and (b) simulated emission spectra of CD(A₂Δ-X₂Π_g) band system obtained from the Ne(³P_{0,2})/C₂D₂ reaction.

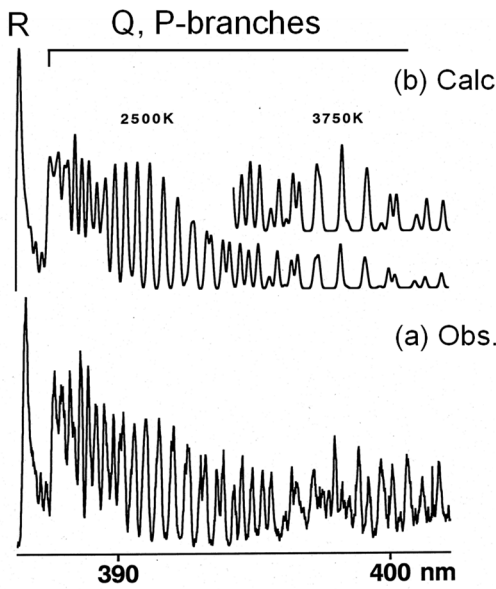


Fig. 3. (a) observed and (b) simulated emission spectra of (0,0) band of CD(B₂Σ-X₂Π_g) band system obtained from the Ne(³P_{0,2})/C₂D₂ reaction.

- the same as those of CD(A). The $\langle E_r \rangle$ and $\langle f_r \rangle$ values of CH(B) are smaller than those of CD(B) by 19–24%.
- (3) The $\langle f_v \rangle + \langle f_r \rangle$ value for CD(A) is 11.5%, whereas that for CD(B) is 8.2%. These results suggest that almost all (89% for CD(A) and 92% for CD(B)) of the total available energies are channeled into

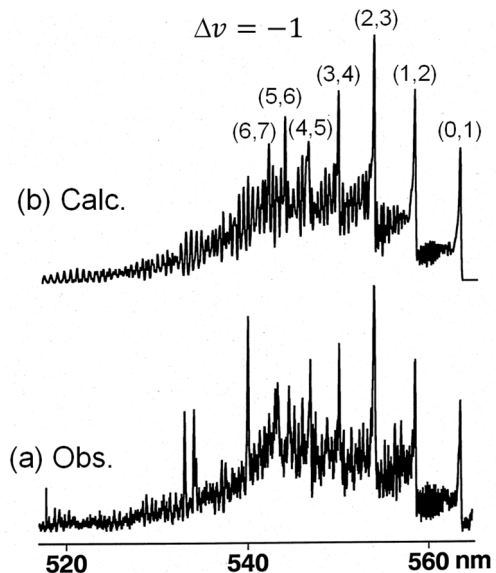


Fig. 4. (a) observed and (b) simulated emission spectra of C₂(d₃Π_g-a₃Π_u) band system obtained from the Ne(³P_{0,2})/C₂D₂ reaction.

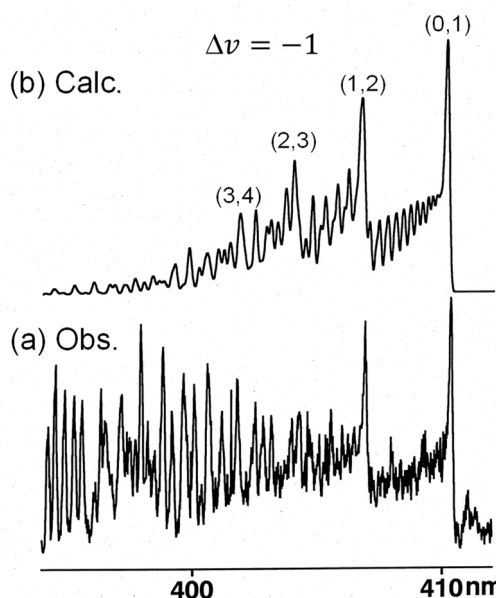


Fig. 5. (a) observed and (b) simulated emission spectra of C₂(C₁Π_g-A₁Π_u) band system obtained from the Ne(³P_{0,2})/C₂D₂ reaction.

rovibrational energies of $\text{CD}(\text{X})$ and relative translational energy of $\text{CD}(\text{A or B}) + \text{CD}(\text{X})$ products, as in the case of CH^* from C_2H_2 .

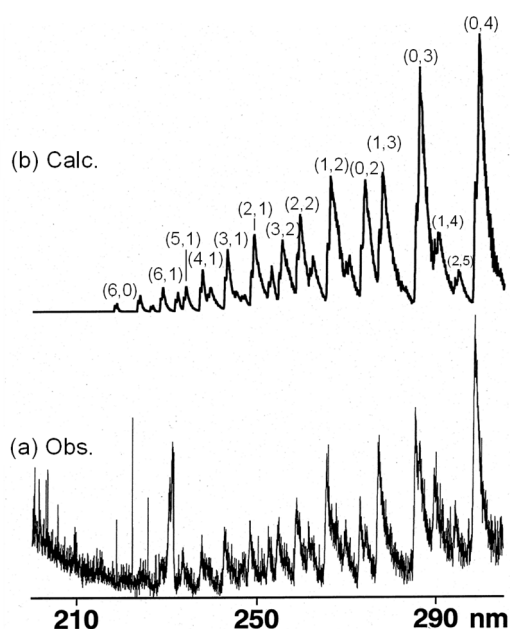


Fig. 6. (a) observed and (b) simulated emission spectra of $\text{C}_2(\text{e}^3\Pi_{\text{g}}-\text{a}^3\Pi_{\text{u}})$ band system obtained from the $\text{Ne}({}^3\text{P}_{0,2})/\text{C}_2\text{D}_2$ reaction.

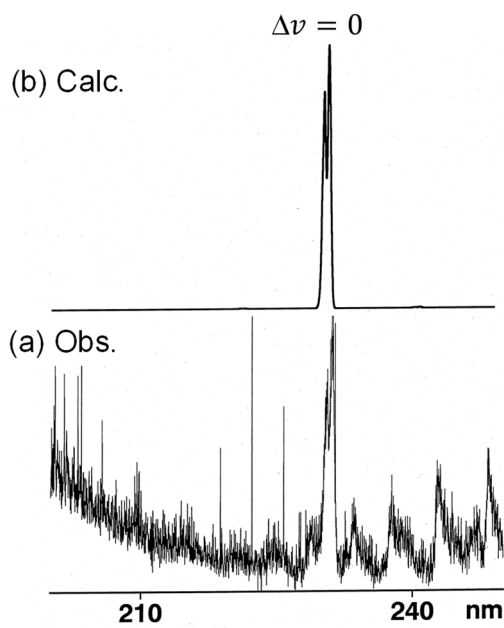


Fig. 7. (a) observed and (b) simulated emission spectra of $\text{C}_2(\text{D}^1\Sigma_{\text{u}}^+-\text{X}^1\Sigma_{\text{g}}^+)$ band system obtained from the $\text{Ne}({}^3\text{P}_{0,2})/\text{C}_2\text{D}_2$ reaction.

(B) Formation of C_2^*

- The vibrational populations of $\text{C}_2(\text{d},\text{C},\text{e},\text{D})$ from C_2D_2 are the same as those from C_2H_2 .¹⁾ The rotational temperatures of $\text{C}_2(\text{d}: v'=0-6)$ from C_2D_2 are higher than those from C_2H_2 by 62–82%, whereas those of $\text{C}_2(\text{C}: v'=0-2)$ are higher than those from C_2H_2 by 10–25%.¹⁾ The rotational temperatures of $\text{C}_2(\text{e}: v'=0-6)$ and $\text{C}_2(\text{D}: v'=0-2)$ are the same as those from C_2H_2 .¹⁾
- The $\langle E_v \rangle$ value of the lowest $\text{C}_2(\text{d})$ state from C_2D_2 is highest (0.53 eV), whereas those of the higher $\text{C}_2(\text{C},\text{e},\text{D})$ states are small (0.12–0.24 eV). The $\langle E_r \rangle$ value of the lowest $\text{C}_2(\text{d})$ state (0.33 eV) is also higher than the other $\text{C}_2(\text{C},\text{e},\text{D})$ states (0.063–0.15 eV).
- The $\langle f_v \rangle$ values for $\text{C}_2(\text{d},\text{C},\text{e},\text{D}) + 2\text{D}$ from C_2D_2 are larger than the $\langle f_r \rangle$ values by factors of 1.4–2.9. These results indicate that deposition of excess energy into vibration is more favorable than that into rotation for the formation of $\text{C}_2^* + 2\text{D}$ from C_2D_2 , as in the case of $\text{C}_2^* + 2\text{H}$ from C_2H_2 .¹⁾
- The $\langle f_v \rangle + \langle f_r \rangle$ values for $\text{C}_2(\text{d},\text{C},\text{e},\text{D}) + 2\text{D}$ from C_2D_2 are 27, 28, 32, and 60%, respectively. The $\text{C}_2\text{H}_2/\text{C}_2\text{D}_2$ ratios of $\langle f_v \rangle + \langle f_r \rangle$ values for $\text{C}_2(\text{d},\text{C},\text{e},\text{D})$ are 0.77–0.90. These results suggest that more excess energies are deposited into vibrational and rotational energies of C_2^* by deuterium substitution.

3.4 Statistical models

As typical examples for the formation of CD^* and C_2^* , the formation dynamics of major $\text{CD}(\text{A})$ and $\text{C}_2(\text{d})$ products from the $\text{Ne}({}^3\text{P}_{0,2})/\text{C}_2\text{D}_2$ system is discussed assuming two-body and three-body dissociation

Table 2. Rovibrational distributions of $\text{CD}(\text{A,B})$ produced from the $\text{Ne}({}^3\text{P}_{0,2})/\text{C}_2\text{D}_2$ reaction. $N_{v'}$ and $P_{v'}^o$ represent observed and calculated prior vibrational distributions, respectively. $P_{v'}^o$ were calculated assuming two-body and three-body dissociation processes.

Emitting species	$v'=0$	$N_{v'}$	$P_{v'}^o$	$P_{v'}^o$	T_r / K
			Two-body	Three-body	
CD(A)	$v'=0$	100	100	100	4200
	$v'=1$	45	77	70	3000
	$v'=2$	8	60	49	800
CD(B)	$v'=0$	100			3125

Table 3. The rovibrational distributions of C₂(d,C,e,D) produced from the Ne(³P_{0,2})/C₂D₂ reaction.

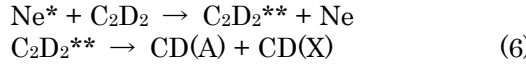
v'	C ₂ (d)			C ₂ (C)			C ₂ (e)			C ₂ (D)		
	$N_{v'}$	$P_{v'}^0$	T_r / K									
0	100	100	5200	100	100	2250	100	100	1000	83	100	800
1	95	81	4500	60	60	1650	60	51	1200	100	9	800
2	88	65	4100	50	33	1250	27	22	700	43	0	450
3	55	51	3500	40	15	1000	12	14	400			
4	63	40	2900				7	7	300			
5	58	30	2500				3	1	300			
6	50	23	2100				1	0	300			

Table 4. Average vibrational and rotational energies (eV) deposited into CD(A,B) or CH(A,B) and average fractions (%) of vibrational and rotational energies deposited into CD(A,B) or CH(A,B) in the Ne(³P₂)/C₂D₂ and Ne(³P₂)/C₂H₂ reactions.

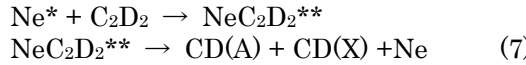
	C ₂ D ₂	C ₂ H ₂	C ₂ H ₂ /C ₂ D ₂
	This work	Ref. 1	
< E_v >	0.10	0.13	1.30
CD(A)	< E_r >	0.32	0.32
or	< f_v >	2.77	3.46
CH(A)	< f_r >	8.75	8.60
	< f_v > + < f_r >	11.52	12.06
	< E_v >	0.0	0.0
CD(B)	< E_r >	0.27	0.22
or	< f_v >	0.0	0.0
CH(B)	< f_r >	8.18	6.21
	< f_v > + < f_r >	8.18	6.21
	< E_v >	0.0	0.0

mechanisms. The same models have been applied to the formation of CH(A,B) and C₂(d,C,e,D) from the Ne(³P₂)/C₂H₂ reaction.¹⁾

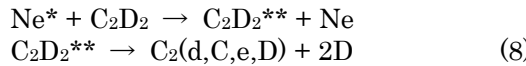
- (a) Two-body dissociation process through resonant excitation transfer



- (b) Three-body dissociation process through resonant excitation transfer



- (c) Three-body dissociation process through resonant excitation transfer

**Table 5.** Average vibrational and rotational energies deposited into C₂(d,C,e,D) and average fractions of vibrational, rotational, and translational energies deposited into C₂(d,C,e,D) in the Ne(³P₂)/C₂D₂ and Ne(³P₂)/C₂H₂ reactions.

	C ₂ D ₂	C ₂ H ₂	C ₂ H ₂ /C ₂ D ₂
	This work	Ref. 1	
< E_v >	0.53	0.53	1.00
< E_r >	0.33	0.19	0.58
C ₂ (d)	< f_v >	16.63	16.01
	< f_r >	10.34	5.75
	< f_v > + < f_r >	26.97	21.76
	< f_t >	73.03	78.24
	< E_v >	0.24	1.00
	< E_r >	0.15	0.13
C ₂ (C)	< f_v >	17.44	16.63
	< f_r >	10.50	8.60
	< f_v > + < f_r >	27.94	25.23
	< f_t >	72.06	74.77
	< E_v >	0.12	1.00
	< E_r >	0.082	0.082
C ₂ (e)	< f_v >	18.62	15.59
	< f_r >	12.88	10.78
	< f_v > + < f_r >	31.50	26.37
	< f_t >	68.50	73.63
	< E_v >	0.18	1.00
	< E_r >	0.063	0.063
C ₂ (D)	< f_v >	44.76	34.38
	< f_r >	15.44	11.86
	< f_v > + < f_r >	60.20	46.24
	< f_t >	39.80	53.76

Statistical vibrational and rotational distributions are calculated for the above three processes using the same equations reported in the preceding paper.¹⁾ As typical examples, the prior vibrational distribution of CD(A: $v'=0-2$)

and rotational distributions of $\text{CD}(\text{A}: v'=0)$ for processes (a) and (b) are calculated and compared with the observed ones in Table 2

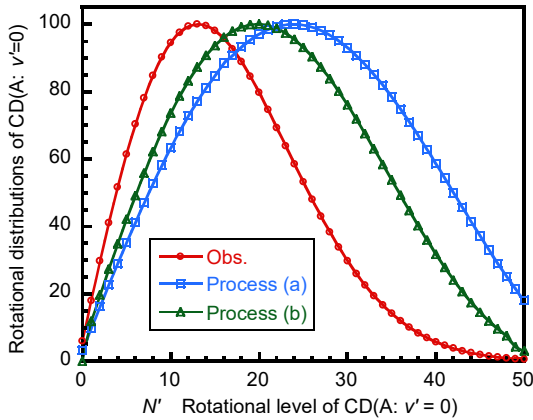
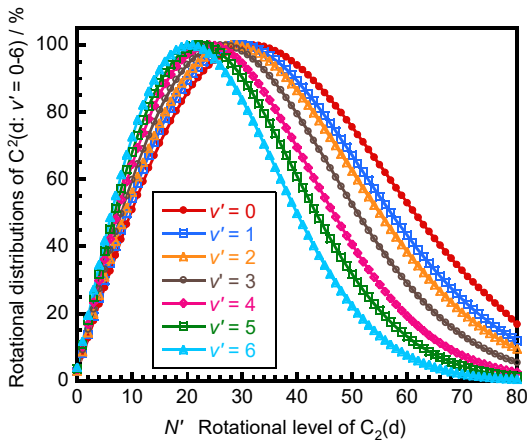


Fig. 8. Observed and two-body and three-body prior rotational distributions of $\text{CD}(\text{A}: v'=0)$ in the $\text{Ne}(^3\text{P}_{0,2})/\text{C}_2\text{D}_2$ reaction.

(a) Obs.



(b) Calc.

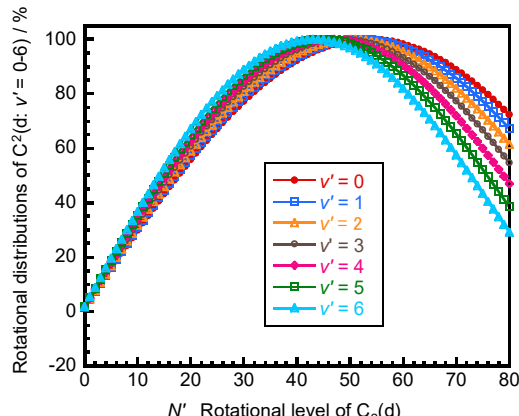


Fig. 9. (a) Observed and (b) calculated three-body prior rotational distributions of $\text{C}_2(\text{d}: v'=0-6)$ in the $\text{Ne}(^3\text{P}_{0,2})/\text{C}_2\text{D}_2$ reaction.

and Fig. 8. The prior vibrational distribution of $\text{CD}(\text{A}: v'=0-2)$ and rotational distributions of $\text{CD}(\text{A}: v'=0)$ predict higher vibrational and rotational excitation than the observed ones for both two-body and three-body dissociation models, as observed in the case of $\text{CH}(\text{A})$ from C_2H_2 .¹⁾

The prior vibrational distributions of $\text{C}_2(\text{d}, \text{C}, \text{e}, \text{D})$ and rotational distributions of $\text{C}_2(\text{d}: v'=0-6)$ calculated for three-body process (c) are compared with the observed ones in Table 3 and Figs. 9a and 9b. It should be noted that the observed vibrational distributions of $\text{C}_2(\text{d}, \text{C}, \text{D})$ are higher than prior ones, whereas a reasonable agreement between the observed and prior distributions is found for $\text{C}_2(\text{e})$. These results are opposite to those of $\text{CD}(\text{A})$, for which the observed vibrational distribution is lower than the prior one. On the other hand, the observed rotational distributions of $\text{C}_2(\text{d}: v'=0-6)$ are lower than prior ones, as in the case of $\text{CD}(\text{A}: v'=0)$. As shown above, similar discrepancies are observed between the observed vibrational and rotational distributions and statistical prior ones for the formation of CD^* or CH^* and C_2^* from C_2D_2 and C_2H_2 .

4. Discussion

4.1 Isotope effects in the $\text{Ne}(^3\text{P}_{0,2})/\text{C}_2\text{H}_2$ and $\text{Ne}(^3\text{P}_{0,2})/\text{C}_2\text{D}_2$ reactions

We found significant deuterium isotope effects on the formation rate constants of CH^* (CD^*) and C_2^* from acetylene. Ibuki et al.^{2,3)} measured isotope effects for the formation of CH^* or CD^* and C_2^* under VUV photoexcitation using NeI lamp and a synchrotron radiation. At photoexcitation energy range of 11.62–11.72 eV, the following ratios have been determined for the emission cross sections, which are proportional to the emission rate constants.

$$k_{\text{H}}(\text{CH}^*)/k_{\text{D}}(\text{CD}^*) = 0.65-0.67 \quad (9\text{a})$$

$$k_{\text{H}}(\text{C}_2^*)/k_{\text{D}}(\text{C}_2^*) = 1.52-1.53 \quad (9\text{b})$$

It should be noted that similar *inverse* deuterium isotope effects are observed between CH^* or CD^* and C_2^* in both $\text{Ne}(^3\text{P}_{0,2})$ excitation and photoexcitation at similar excitation energies. However, the isotope effect on CH^* obtained in the $\text{Ne}(^3\text{P}_{0,2})$ excitation is smaller than that in VUV photoexcitation, whereas that on C_2^* is larger than that in VUV photoexcitation.

According to a simple RRKM theory,^{3,6)}

kinetic hydrogen isotope effects for the formation of CH* or CD* and C₂ from C₂H₂ and C₂D₂ are expressed as follows.

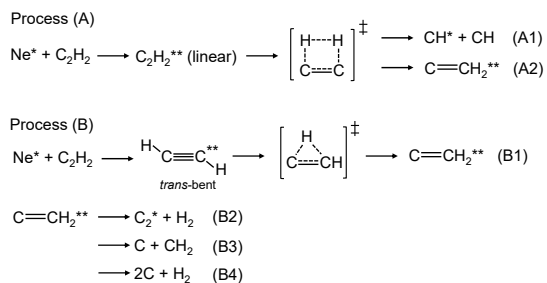
$$k_H(CH^*)/k_D(CD^*) = (\mu_{C-CD}/\mu_{C-CH})^{1/2} = 1.02 \quad (10a)$$

$$k_H(C_2^*)/k_D(C_2^*) = (\mu_{C-D}/\mu_{C-H})^{1/2} \times (\mu_{C-D}/\mu_{C-H})^{1/2} = \mu_{C-D}/\mu_{C-H} = 1.86 \quad (10b)$$

Here, μ is the reduced mass. The observed isotope ratio for C₂* in the Ne(³P_{0,2}) reaction, 1.73, is in reasonable agreement with the calculated value from Eq. 10b (1.86). It seems therefore reasonable to assume that the observed isotope effect on C₂* in the Ne(³P_{0,2}) reaction originates from normal kinetic isotope effect between C–H and C–D bond scissions, which is independent on the spin-multiplicity of the precursor superexcited states.

The *inverse* isotope effect between CH and CD cannot be explained by the RRKM theory, which gives a larger value above 1. To explain the *inverse* isotope effects on C₂* and CH* or CD*, Ibuki et al.³⁾ proposed two different mechanisms below 80 nm (>15.50 eV) and above 80 nm (<15.50 eV) region. The primarily important effect at the wavelength below 80 nm is the hydrogen isotope effect in the C–H and C–D bond dissociation which causes $k_H(C_2^*) > k_D(C_2^*)$. Because of the competition with these C–H and C–D bond dissociation channels, the processes leading to CH* and CD* radicals show an *inverse* isotope effect. They proposed four-membered cyclic isomer (Process A in Scheme 1), as one of the intermediate structures. The CC bond dissociation (A1) and the isomerization (A2) compete in the four-membered cyclic isomer. The probability of H atom migration in reaction (A2) should be higher than that of D atom due to the tunneling effect across the energy barrier. After the formation of C=CH₂** vinylidene, dissociation to C₂* (B2) and the dark reactions (B3) and (B4) occur competitively, as shown in process B in Scheme 1. Dark dissociation processes (B3) and (B4) are more important for C₂H₂** because of faster formation rate of C=CH₂**. The fact that the more C=CH₂** formation the weaker emission of CH* causes the *inverse* hydrogen isotope effect between the $k_H(CH^*)$ and $k_D(CD^*)$ values.

At the wavelengths longer than 80 nm, the dark processes (B3) and (B4), which are initiated by the isomerization via a *trans*-bent superexcited state to vinylidene, become important (Process B in Scheme 1). A tunneling



Scheme 1. Possible decomposition scheme of C₂H₂** in the Ne(³P_{0,2})/C₂H₂ reaction.

effect on the H and D migration in the intermediates causes the *inverse* hydrogen isotope effect on the CH* and CD* emission intensities because the more C=CH₂** formation the weaker CH* emission.

In the Ne(³P_{0,2}) reaction, precursor C₂H₂** superexcited states of CH* and C₂* are triplet Rydberg states, which are different from singlet Rydberg states formed under VUV photoexcitation. However, it is reasonable to assume that similar mechanisms as proposed to explain isotope effects under VUV photoexcitation are involved in the Ne(³P_{0,2}) reaction. In the case of photoexcitation, C₂H₂ molecules are excited into a single resonant state with the same energy as that of incident photons. According to our systematic FA optical spectroscopic studies on energy-transfer reactions of rare gas metastable Ar(³P_{0,2}), Kr(³P_{0,2}), and Xe(³P_{0,2}) atoms with such small molecules as N₂ and CO, energy-transfer from Rg(³P_{0,2}) to molecules occurs near resonantly in most cases, where a few selective vibrational levels of triplet states are formed.⁷⁻¹²⁾ However, there was an exceptional case, where a wide vibrational distribution involving off-resonance states has been observed (e.g. Kr(³P_{0,2}) + N₂ → N₂(B³Π_g:v'=3-12) + Kr).¹³⁾ Therefore, we cannot exclude the possibility of the formation of several triplet C₂H₂** or C₂D₂** states with wide energy distributions in the Ne(³P_{0,2}) reaction. If products in wide energy distributions are formed, more than one mechanism will take part in the observed *inverse* isotope effect on CH* and CD*.

In our previous paper on the Ne(³P_{0,2})/C₂H₂ reaction,¹⁾ we concluded that CH(A,B) and C₂(d,C,e,D) are formed via *trans*-bent near-resonant $np\pi^* \leftarrow 3\sigma_g$ Rydberg states converging to the first excited $\tilde{\Lambda}$ 2A_g state of C₂H₂⁺. Non-linear precursor superexcited states with enlarged C≡C bond and excited CCH bending vibration led to vibrational excitation of C₂* and rotational excitation of

CH^* and C_2^* radicals. It has been reported that the *trans*-bent $\text{C}_2\text{H}_2^+(\tilde{\Lambda}^2A_g)$ ion generated at $\text{hv}>16.351$ eV (75.8 nm) is unimolecularly rearranged into the $\tilde{\Lambda}^2A_1$ state of vinylidene $\text{C}=\text{CH}_2^+$ ion.¹⁴⁾ The rearrangement to vinylidene, reaction (B1), is highly probable in the neutral superexcited acetylene, especially in its Rydberg states converging to *trans*-bent $\text{C}_2\text{H}_2^+(\tilde{\Lambda}^2A_g)$ ion. Because of faster tunneling effect on the H and D migration in the intermediates, the more $\text{C}=\text{CH}_2^{**}$ formation causes the slower formation rate of CH^* . Based on this fact, direct dissociation of *trans*-bent $\text{C}_2\text{H}_2^{**}$ and $\text{C}_2\text{D}_2^{**}$ into CH^* and CD^* completes with rearrangement to vinylidene form, which suppresses the CH^* formation.

In the $\text{Ne}(^3\text{P}_{0,2})$ reaction, not only isomerization from *trans*-bent to three-membered cyclic transition state (B1) as described above, but also isomerization to non-linear four-membered cyclic isomer leading to the $\text{C}=\text{CH}_2^{**}$ formation (A2) may contribute to the *inverse* isotope effect between CH^* and CD^* . The formation of such non-linear intermediates with a loosen $\text{C}\equiv\text{C}$ bond may also be one reason for the occurrence of high vibrational excitation of C_2^* and high rotational excitation of CH^* and C_2^* . Further detailed experimental and theoretical studies on molecular structures and dissociation processes of high energy triplet Rydberg states are required to determine the relative importance of the above explanations for the *inverse* isotope effect for CH^* (CD^*) in the $\text{Ne}(^3\text{P}_{0,2})$ reaction.

5. Summary and Conclusion

Isotope effects for the formation of CH^* or CD^* and C_2^* from the energy-transfer reactions of $\text{Ne}(^3\text{P}_{0,2})$ with C_2H_2 and C_2D_2 have been studied in the Ne flowing afterglow. The emission rate constants of CD(A,B,C) and $\text{C}_2(\text{d,C,e,D})$ in the $\text{Ne}(^3\text{P}_{0,2})/\text{C}_2\text{D}_2$ reaction were determined. The isotopic ratios of $k_{\text{H}}(\text{CH}^*)/k_{\text{D}}(\text{CD}^*)$ and $k_{\text{H}}(\text{C}_2^*)/k_{\text{D}}(\text{C}_2^*)$ were determined to be 0.85 and 1.73, respectively. The positive isotope effect for C_2^* was consistent with that predicted from the RRKM theory because dissociation rate of C–H bond is faster than that of C–D bond. On the other hand, negative isotope effect for CH^* (or CD^*) does not agree with the prediction from the RRKM theory. It was explained by the fact that the formation of CH^* or CD^* competes with that of C_2^* from dissociation of C–H bonds, so

that faster dissociation of C–H bonds than C–D bonds suppresses the formation of CH^* . Other possible mechanisms to explain the *inverse* isotope effect on CH^* and CD^* were proposed.

The nascent vibrational and rotational distributions of $\text{CD(A: } \nu'=0-2, \text{B: } \nu'=0)$ and $\text{C}_2(\text{d: } \nu'=0-6, \text{C: } \nu'=0-3, \text{e: } \nu'=0-6, \text{D: } \nu'=0-2)$ were determined. The vibrational distributions of CD(A,B) and $\text{C}_2(\text{d,C,e,D})$ from the $\text{Ne}(^3\text{P}_{0,2})/\text{C}_2\text{D}_2$ reaction were similar to those from the $\text{Ne}(^3\text{P}_{0,2})/\text{C}_2\text{H}_2$ reaction. The rotational temperatures of CD(A,B) were also similar to those of CH(A,B) . The rotational temperatures of the lower $\text{C}_2(\text{d,C})$ states from the $\text{Ne}(^3\text{P}_{0,2})/\text{C}_2\text{D}_2$ reaction were higher than those from the $\text{Ne}(^3\text{P}_{0,2})/\text{C}_2\text{H}_2$ reaction. On the other hand, the rotational temperatures of the higher $\text{C}_2(\text{e,D})$ states from the $\text{Ne}(^3\text{P}_{0,2})/\text{C}_2\text{D}_2$ reaction were the same as those from the $\text{Ne}(^3\text{P}_{0,2})/\text{C}_2\text{H}_2$ reaction.

Acknowledgments

This work was supported by the Mitsubishi foundation (1996) and JSPS KAKENHI Grant number 09440201 (1997-2000).

References

- 1) M. Tsuji, T. Komatsu, K. Uto, J.-I. Hayashi, and T. Tsuji, *Engineering Sciences Reports, Kyushu University*, 43, 8 (2021).
- 2) T. Ibuki and Y. Horie, *Chem. Phys. Lett.*, 196, 541 (1992).
- 3) T. Ibuki, Y. Horie, A. Kamiuchi, Y. Morimoto, M. C. K. Tinone, K. Tanaka, and K. Honma, *J. Chem. Phys.*, 102, 5301 (1995).
- 4) *NIST Chemistry WebBook*, NIST Standard Reference Database, Number 69 (2018): <http://webbook.nist.gov/chemistry>.
- 5) K. P. Huber and G. Herzberg, “*Molecular Spectra and Molecular Structure, IV. Constants of Diatomic Molecules*”, Van Nostrand Reinhold, New York (1979).
- 6) B. S. Rabinovitch and D. W. Setser, “*Advances in Photochemistry*, Vol. 3”, Interscience, New York (1964) p. 1.
- 7) M. Tsuji, K. Yamaguchi, S. Yamaguchi, and Y. Nishimura, *Chem. Phys. Lett.*, 143, 482 (1988).
- 8) M. Tsuji, K. Yamaguchi, and Y. Nishimura, *Chem. Phys.*, 123, 151 (1988).
- 9) M. Tsuji, K. Yamaguchi, and Y. Nishimura, *Chem. Phys.*, 125, 337 (1988).
- 10) M. Tsuji, K. Yamaguchi, H. Obase, and Y. Nishimura, *Chem. Phys. Lett.*, 161, 41 (1989).
- 11) M. Tsuji, K. Yamaguchi, H. Kouno, and Y. Nishimura *Jpn. J. Appl. Phys.*, 30, 1281 (1991).
- 12) M. Tsuji, K. Yamaguchi, M. Kikukawa, H. Kouno, T. Funatsu, and Y. Nishimura, *Bull. Chem. Soc. Jpn.*, 65, 1713 (1992).
- 13) M. Tsuji, K. Yamaguchi, and Y. Nishimura *J. Chem. Phys.*, 89, 3391 (1988).
- 14) P. Rosmus, P. Botshwina, and J. P. Maier, *Chem. Phys. Lett.*, 84, 71 (1981).